1 **Molecular Cancer Therapeutics (Models & Technologies)**

2 **Targeting tumor neoangiogenesis via targeted adenoviral vector to achieve**

3 **effective cancer gene therapy for disseminated neoplastic disease**

4 Myungeun Lee[1], Zhi Hong Lu[1], Jie Li[1], Elena A. Kashentseva[1], Igor P. Dmitriev[1], Samir A.

5 Mendonca[1] and David T.Curiel[1,2*]

6 [1]Division of Cancer Biology, Department of Radiation Oncology, School of Medicine,

7 Washington University in St. Louis, St. Louis, MO 63110, USA

8 [2]Biologic Therapeutics Center, Department of Radiation Oncology, School of Medicine,

9 Washington University in St. Louis, St. Louis, MO 63110, USA

10

11 **Contact Information: Address for correspondence***

12 David T. Curiel, MD, Ph.D., Distinguished Professor of Radiation Oncology

13 Director, Biologic Therapeutics Center

14 Washington University in St. Louis, School of Medicine,

15 660 South Euclid Avenue, Campus Box 8224, St. Louis, MO 63110, USA

16 Phone: 314.747.5443, Fax: +82-31-8018-8014

17 Email: dcuriel@wustl.edu

18 **List of Abbreviations:** Adenoviral Vectors (Ad), Therapeutic Index (TI), Herpes Simplex Virus

19 thymidine kinase (HSV*tk*), Ganciclovir (GCV), Roundabout Guidance Receptor 4 (ROBO4),

20 Renal Cell Carcinoma (RCC)

21 **Running Title:** Triple targeted adenoviral vector for cancer gene therapy

ABSTRACT

The application of cancer gene therapy has heretofore been restricted to local, or locoregional, neoplastic disease contexts. This is owing to the lack of gene transfer vectors which embody the requisite target cell selectivity in vivo required for metastatic disease applications. To this end, we have explored novel vector engineering paradigms to adapt adenovirus for this purpose.

Our novel strategy exploits three distinct targeting modalities that operate in functional synergy. Transcriptional targeting is achieved via the hROBO4 promoter, which restricts transgene expression to proliferative vascular endothelium. Viral binding is modified by incorporation of an RGD4C peptide in the HI loop of the fiber knob for recognition of cellular integrins. Liver sequestration is mitigated by ablation of Factor X binding to the major capsid protein hexon by a serotype swap approach. The combination these technologies into the context of a single vector agent represents a highly original approach. Studies in a murine model of disseminated cancer validated the in vivo target cell selectivity of our vector agent. Of note, clear gains in therapeutic index accrued these vector modifications.

Whereas there is universal recognition of the value of vector targeting, very few reports have validated its direct utility in the context of cancer gene therapy. In this regard, our report validates the direct gains which may accrue these methods in the stringent delivery context of disseminated neoplastic disease. Efforts to improve vector targeting thus represent a critical direction to fully realize the promise of cancer gene therapy.

INTRODUCTION

41

42 A wide range of strategies have been developed to apply gene therapy to the context of

43 neoplastic disease (1-4). The central goal embodied in these molecular interventions is the

44 achievement of an improved therapeutic index compared to conventional cancer therapies.

45 Heretofore, such *in vivo* cancer gene therapies have been applied for local, or locoregional,

46 neoplastic disease. This is owing to the fact that currently available gene transfer vectors lack

47 the *in vivo* target cell selectivity mandated for the clinical context of disseminated disease.

48 In this regard, there has been a field-wide recognition of the need for gene transfer vectors

49 which embody the capacity for target cell selectivity (5). Indeed, an NIH report on gene therapy

50 highlighted this goal as the highest mandate for the field. For cancer, such a vector targeting

51 capacity thus represents the *sine qua non* for practical advancement of these promising

52 strategies to the problematic clinical setting of metastatic disease. Given this consideration, the

53 paucity of reports of the successful application of vector targeting for cancer gene therapy is

54 noteworthy.

55 To this end, we have endeavored modification of adenoviral vectors (Ad) to address this key

56 gene delivery mandate. Based on the unique molecular promiscuity of the parent virus, we

57 hypothesized that targeting might be achieved exploiting multiple biologic axes. Further, we

58 sought to combine such distinct targeting strategies to realize functional synergy vis-à-vis the

59 achievement of target cell selectivity. On this basis, the requirement for *in vivo* selectivity, in the

60 context of disseminated neoplastic disease, might be achieved.

3

MATERIALS AND METHODS

Adenovirus production

The replication incompetent E1-deleted Ad5 vectors used for study were prepared using a two-plasmid cloning method. Untargeted or triple targeted Ad5 encoding the GFP reporter gene or the HSVtk therapeutic gene were produced in accordance with the standard techniques (6). Briefly, adenoviral genome-including plasmids were digested with PacI for releasing the recombinant viral genomes, and transfected into HEK293 cells. Rescued viruses was serially amplified, and then purified by centrifugation on CsCl gradients according to standard protocols. For in vitro and in vivo study, viruses were dialyzed against phosphate-buffered saline (PBS) containing 10% glycerol, and stored at −80°C. The titers of physical viral particles (vp) were determined by methods described by Maizel et al.(7).

In *vitro* validation of adenovirus

HUVEC (Human primary endothelial), bEnd-3 (Mouse primary endothelial) and NIH/3T3 (mouse embryonic fibroblast) cells were obtained from the ATCC and maintained for assays according to the manufacturer's instructions. Total expression levels of HSVtk proteins in whole cell lysate were determined with anti-tk antibody (kindly provided by Dr. Summers) by western blot analysis in accordance with the standard protocols. For HSVtk/GCV killing activity assay, cells were infected with virus encoding either GFP or HSVtk gene, ganciclovir (Selleckchem) prodrug was administered to cells via serial diluted drug concentration. To measure the cellular ATP contents (Promega) as a marker for cell viability, assay plates were read in a microplate luminometer (Berthold detection system) and cell viability was analyzed. Dose-response curve (DRC) analysis curves were plotted by Graph Pad Prism v7.0c software.

4

Murine xenograft models

83

84 Triple immunodeficient NOD/SCID/IL2Rγ (NSG) mice were injected subcutaneously with $1x10^6$

85 786-0 renal carcinoma cells (mCherry expressed cell line). Two weeks later the mice were

86 intravenously injected with $1x10^{11}$ vp of un-targeted Ad5.CMV.GFP or triple targeted Ad-GFP

87 viruses. To perform histopathological analysis in tumor or organs, mice were sacrificed under

88 anesthesia (Avertin, Sigma-Aldrich) at three days post-virus injection. The tumor bearing tissues

89 were harvested, followed by post-fixed in 4% paraformaldehyde for 2 hours at room

90 temperature, cryopreserved in 30% sucrose for 16 hours at 4ºC, and cryo-embedded in NEG50

91 (Thermo Fisher Scientific) over 2-methylbutane/liquid nitrogen. Histopathological images were

92 captured by epifluorescence microscopy. To perform histopathological analysis in SPC6

93 subcutaneous tumor, all assay procedures were conducted in accordance with same protocols.

Tissue harvest and Immunofluorescence staining

94

95 Mice were administrated with $1x10^{11}$ VP of triple targeted Ad via tail-vein injection. Three days

96 post virus infection, mice were anesthetized and tissues (Liver, Lung, Pancreas, Spleen,

97 Kidney, Small Bowel, Heart, Muscle and Brain) harvested for immunofluorescence staining. For

98 frozen sections, organ slices were cryo-preserved in 30% sucrose in PBS at 4^oC overnight,

99 embedded in NEG50 mounting medium (Thermo Fisher Scientific), and then frozen in a liquid

100 nitrogen pre-chilled 2-methylbutane containing bucket. Sectioning of frozen organs was carried

101 out using the CryoJane taping system (Leica Biosystems Inc). All frozen section slides were

102 subject to immunofluorescence staining analysis in accordance with the standard techniques

103 (8). Primary antibodies used in this study included hamster anti-CD31 (EMD Millipore), rat anti-

104 endomucin (eBioscience), rat anti-PDGFRβ (eBioscience), rabbit anti-HSVtk (Dr. Summers's

105 lab) and Alexa Fluor 488 or 594-conjugated secondary antibodies (Jackson ImmunoResearch

106 Laboratories).

5

107 **Animal studies for therapeutic index gains**

108 Triple immunodeficient NSG mice allow for modeling of all metastatic sites as published

109 previously (8,9). For systemic metastases, mice was injected intracardially with 5×10^5 786-0

110 renal carcinoma cells (Luciferase gene expressed). Tumor growth was monitored and quantified

111 using bioluminescence imaging (BLI) analysis. Three weeks after tumor implantation, mice were

112 intravenously injected via tail vein with 1×10^{11} vp of each virus. During the following 7 days,

113 mice received daily intraperitoneal injection of GCV (50mg/kg/7days) according to the different

114 treatment groups ([n=8 mice/group]: un-targeted Ad5-GFP, un-targeted Ad5-HSVtk and triple

115 targeted Ad-HSVtk plus GCV). All mice in each group were monitored for body weight during

116 the treatment time and compared the survival time. For study of tumor progression, final ROI

117 values were monitored and compared (Increased fold=last ROI value/initial ROI value) in the

118 survival mice. Survival data was plotted on a Kaplan-Meier curve in all animal groups by Graph

119 Pad Prism v7.0c software. The studied was terminated at 8 weeks (56 days post-tumor

120 implantation) according to approved protocols and pursuant to NIH guidelines for the care and

121 use of laboratory animals standards. All animal experiments were reviewed and approved by

122 the Institutional Animal Care and Use Committee of the Washington University in Saint Louis,

123 School of Medicine (protocol #.20160292).

124   **RESULTS**

125   **Generated triple targeting vector for gene therapy**

126   As the main limit to the systemic employment of Ad is liver sequestration (10), we first sought to

127   address this issue. Our studies, and those of others, had linked this phenomenon to vector

128   capsid association with serum factor X (11,12). On this basis, we employed a strategy of capsid

129   chimerism whereby the major capsid protein hexon of the serotype 5 vector base was

130   substituted with a cognate from the alternate human adenovirus serotype 3. We had previously

131   shown that this modification substantially mitigated sequestration in the reticuloendothelial

132   system (RES) in the context of systemic vector administration (12,13). This liver "un-targeting"

133   method was then combined with modifications designed to direct the expression of delivered

134   transgenes to tumor vascular endothelium. Specific vector particle binding was enhanced for the

135   target cells by the incorporation into the Ad capsid fiber knob of the RGD4C peptide (14,15).

136   This ligand exhibits preferentiality for integrins of $\alpha_v\beta_3$ and $\alpha_V\beta_3$ class over-expressed in

137   angiogenic endothelium. This approach was also combined with a transcriptional targeting

138   strategy to restrict transgene expression target cells. In this case, the promoter of the

139   roundabout guidance receptor 4 (ROBO4) gene, which is selectively inductive for proliferative

140   endothelium, was employed. We hypothesized that the combination of the liver un-targeting and

141   vector targeting methods (**Fig. 1**) would provide functional synergy with respect to the

142   achievement of the *in vivo* selectivity mandated for disseminated neoplastic disease cancer

143   gene therapy.

144   **Evaluated vector for cancer gene therapy**

145   Such a triple targeted Ad was thus constructed to achieve expression of the HSVtk therapeutic

146   gene selectively within proliferative tumor endothelium *in vitro*. This gene has been applied

147   historically for molecular chemotherapy cancer gene therapy approaches (16,17). Its

7

148 employment here thus served to reconcile our findings with the extensive literature relating to

149 the use of HSVtk for cancer gene therapy. After rescue and upscale, the virion was subject to

150 genomic analysis (**Fig. 2A**). This study confirmed that the control un-targeted adenovirus, and

151 the triple targeted adenovirus, both contained the cassette with the HSVtk therapeutic gene.

152 Infection of human endothelial cells (HUVEC), with follow-on Western blot analysis, confirmed

153 expression of HSVtk in cells infected via both vectors (**Fig. 2B**). Next, analysis of the specificity

154 of expression was carried-out utilizing an *in vitro* assay whereby HSVtk expression sensitized

155 cells to the cytotoxic effects of GCV. Target cells were human endothelial (HUVEC) or murine

156 endothelial cells (bEnd-3). In this analysis, it could be seen that the target cells were sensitive to

157 vector-mediated cytotoxicity exclusively after infection with the triple targeted Ad encoding

158 HSVtk (**Fig. 2C**), under GCV treatment. In addition, regarding to the transduction efficacy, we

159 confirmed with NIH/3TC cells (mouse embryonic fibroblast) including demonstration of the target

160 cells specificity (**Fig. 2D**). These studies thus validated the endothelial selectivity of our vector

161 targeting schema.

162 **Advanced vector targeting to tumor *in vivo***

163 We next sought to validate the *in vivo* selectivity of our vector methods in a systemic delivery

164 context. For this analysis, we derived versions of the control and triple targeted adenovirus

165 which encoded the GFP reporter gene. Immunodeficient NOD/SCID/IL2Rγ (NSG) mice were

166 xenografted with subcutaneous nodules of the human renal carcinoma cell line 786-0 (8).

167 Animals were then challenged with 1×10^{11} particles of the control and targeted Ad with analysis

168 of harvested tumor and organs at 3 days later. As the major site for ectopic Ad localization is the

169 liver, analysis was limited to this site and target tumor. In these studies it could be seen that

170 untargeted Ad was largely sequestered in the liver, with no detectable reporter noted within

171 vascular areas of the tumor (**Fig. 3A**). In marked contrast, the triple targeted Ad avoided ectopic

8

172   localization within the liver and spleen. Of note, high levels of reporter gene were seen within

173   the harvested subcutaneous tumor nodules via secondary staining analysis confirmed the

174   identity of gene modified cells as tumor endothelium (**Fig 3B**). Our findings confirm that the

175   hexon modification of our triple targeted Ad achieves the desired goal of liver un-targeting,

176   without the accrual of major new sites of ectopic gene delivery (**Fig. 3C**). Furthermore, as an

177   even more stringent model (xenografted with subcutaneous nodules of the syrian golden

178   hamster pancreatic carcinoma cell line SHPC6), it could be seen the targeting specificity of our

179   triple targeted adenovirus in the context of other tumors (**Fig. 3D**). Thus, our triple targeting

180   strategy achieves highly specific *in vivo* selectivity.

181   **Improved vector to achieve the therapeutic index gains in *vivo***

182   Lastly, we endeavored evaluation of the therapeutic index gains which accrue synergistic

183   targeting. The therapy experiment with targeted adenovirus (vs. non-targeted adenovirus) was

184   employed in a murine model of metastatic disease. The triple targeting specificity mitigated the

185   vector-associated toxicity known to be associated with the systemic application of un-targeted

186   Ad encoding HSVtk (18) (**Fig. 4A**). In parallel with that, of note, it could be seen that extended

187   survival time accrued to the treatment group that received only the triple targeted Ad encoding

188   HSVtk with significant differences [**$p<0.005$] (**Fig. 4C**). Our demonstration of antitumor therapy

189   was accomplished in a context more stringent than that required only for local control, however,

190   it could be seen the potential for improvement the therapeutic effect (**Fig. 4B**). Also, It could be

191   seen the persistence of the vector in the metastatic tumor as well**.** These finding demonstrated

192   directly the improved therapeutic index which accrued the employed of vector targeting for this

193   established cancer gene therapy approach.

9

194   **DISCUSSION**

195   Our study highlights the direct benefits that may derive from the application of vector targeting

196   methods to the context of cancer gene therapy. In this regard, in vivo cancer gene therapies

197   have been restricted to local diseases contexts owing to the limits of currently available gene

198   transfer vectors. Thus, the problematic clinical context of metastatic cancer has not been

199   addressable to this point via gene therapy methods. Further in this regard, the universal

200   recognition of the potential value of vector targeting has not been translated to the context of

201   cancer gene therapy studies demonstrating therapeutic gains. The advent of our novel vector

202   targeting technology now provides adequate selectivity in vivo to test this hypothesis of field-

203   wide significance. Our early finding reported here thus provide the rationale for future studies

204   designed to apply cancer gene therapy to this problematic clinical context most warranties novel

205   interventions.

10

206 **Disclosure of potential conflicts of interest**

207 No potential conflicts of interest were disclosed.

208 **Authors' contributions**

209 ME.L, Z.H.L and D.T.C formulated and designed the project. E.K and I.D. advice the critical

210 experiments and S.M provided the critical materials. Z.H.L and J.L. aided critical figures

211 generation and assisted the histopathological images *in vivo* study. ME.L and Z.H.L, contributed

212 to all experiments and figure generation for manuscript. ME.L. and D.T.C wrote the manuscript

213 with input from all authors for data interpretation.

214 **Acknowledgements**

11

221 **REFERENCES**

222 1. Hsiao WC, Sung SY, Chung LWK, Hsieh CL. Osteonectin Promoter-Mediated Suicide Gene
223   Therapy of Prostate Cancer. Methods Mol Biol **2019**;1895:27-42 doi 10.1007/978-1-4939-8922-
224   5_3.
225 2. Sun W, Shi Q, Zhang H, Yang K, Ke Y, Wang Y, *et al.* Advances in the techniques and
226   methodologies of cancer gene therapy. Discov Med **2019**;27(146):45-55.
227 3. Yamamoto Y, Nagasato M, Yoshida T, Aoki K. Recent advances in genetic modification of
228   adenovirus vectors for cancer treatment. Cancer Sci **2017**;108(5):831-7 doi 10.1111/cas.13228.
229 4. Piccolo P, Brunetti-Pierri N. Challenges and Prospects for Helper-Dependent Adenoviral Vector-
230   Mediated Gene Therapy. Biomedicines **2014**;2(2):132-48 doi 10.3390/biomedicines2020132.
231 5. Baker AH, Kritz A, Work LM, Nicklin SA. Cell-selective viral gene delivery vectors for the
232   vasculature. Exp Physiol **2005**;90(1):27-31 doi 10.1113/expphysiol.2004.028126.
233 6. Chartier C, Degryse E, Gantzer M, Dieterle A, Pavirani A, Mehtali M. Efficient generation of
234   recombinant adenovirus vectors by homologous recombination in Escherichia coli. J Virol
235   **1996**;70(7):4805-10.
236 7. Sweeney JA, Hennessey JP, Jr. Evaluation of accuracy and precision of adenovirus absorptivity at
237   260 nm under conditions of complete DNA disruption. Virology **2002**;295(2):284-8 doi
238   10.1006/viro.2002.1406.
239 8. Lu ZH, Kaliberov S, Sohn RE, Kaliberova L, Du Y, Prior JL, *et al.* A new model of multi-visceral and
240   bone metastatic prostate cancer with perivascular niche targeting by a novel endothelial specific
241   adenoviral vector. Oncotarget **2017**;8(7):12272-89 doi 10.18632/oncotarget.14699.
242 9. Lu ZH, Kaliberov S, Sohn RE, Kaliberova L, Curiel DT, Arbeit JM. Transcriptional targeting of
243   primary and metastatic tumor neovasculature by an adenoviral type 5 roundabout4 vector in
244   mice. PLoS One **2013**;8(12):e83933 doi 10.1371/journal.pone.0083933.
245 10. Rojas LA, Moreno R, Calderon H, Alemany R. Adenovirus coxsackie adenovirus receptor-
246   mediated binding to human erythrocytes does not preclude systemic transduction. Cancer Gene
247   Ther **2016**;23(12):411-4 doi 10.1038/cgt.2016.50.
248 11. Lopez-Gordo E, Denby L, Nicklin SA, Baker AH. The importance of coagulation factors binding to
249   adenovirus: historical perspectives and implications for gene delivery. Expert Opin Drug Deliv
250   **2014**;11(11):1795-813 doi 10.1517/17425247.2014.938637.
251 12. Short JJ, Rivera AA, Wu H, Walter MR, Yamamoto M, Mathis JM, *et al.* Substitution of adenovirus
252   serotype 3 hexon onto a serotype 5 oncolytic adenovirus reduces factor X binding, decreases
253   liver tropism, and improves antitumor efficacy. Mol Cancer Ther **2010**;9(9):2536-44 doi
254   10.1158/1535-7163.Mct-10-0332.
255 13. Kaliberov SA, Kaliberova LN, Hong Lu Z, Preuss MA, Barnes JA, Stockard CR, *et al.* Retargeting of
256   gene expression using endothelium specific hexon modified adenoviral vector. Virology
257   **2013**;447(1-2):312-25 doi 10.1016/j.virol.2013.09.020.
258 14. Bilbao G, Contreras JL, Dmitriev I, Smyth CA, Jenkins S, Eckhoff D, *et al.* Genetically modified
259   adenovirus vector containing an RGD peptide in the HI loop of the fiber knob improves gene
260   transfer to nonhuman primate isolated pancreatic islets. Am J Transplant **2002**;2(3):237-43.
261 15. Wang M, Hemminki A, Siegal GP, Barnes MN, Dmitriev I, Krasnykh V, *et al.* Adenoviruses with an
262   RGD-4C modification of the fiber knob elicit a neutralizing antibody response but continue to
263   allow enhanced gene delivery. Gynecol Oncol **2005**;96(2):341-8 doi
264   10.1016/j.ygyno.2004.09.063.

12

265   16.   Wildner O, Morris JC, Vahanian NN, Ford H, Jr., Ramsey WJ, Blaese RM. Adenoviral vectors
266   capable of replication improve the efficacy of HSVtk/GCV suicide gene therapy of cancer. Gene
267   Ther **1999**;6(1):57-62 doi 10.1038/sj.gt.3300810.
268   17.   Hodish I, Tal R, Shaish A, Varda-Bloom N, Greenberger S, Rauchwerger A*, et al.* Systemic
269   administration of radiation-potentiated anti-angiogenic gene therapy against primary and
270   metastatic cancer based on transcriptionally controlled HSV-TK. Cancer Biol Ther **2009**;8(5):424-
271   32 doi 10.4161/cbt.8.5.7589.
272   18.   Yi QY, Bai ZS, Cai B, Chen N, Chen LS, Yuan T*, et al.* HSVTK/GCV can induce cytotoxicity of
273   retinoblastoma cells through autophagy inhibition by activating MAPK/ERK. Oncol Rep
274   **2018**;40(2):682-92 doi 10.3892/or.2018.6454.

275

13

276   **FIGURE LEGENDS**

277   **Figure 1. Schema of 'triple-targeted' genetic modifications of adenovirus to accomplish**

278   ***in vivo* targeting of tumor endothelium.** Liver un-targeting has previously been accomplished

279   via genetic modification of hexon domains that can associate with serum factor X. Hexon

280   ectodomain hypervariable regions (HVR7) of the vector was replaced base human adenovirus

281   serotype 5 with the corresponding domains from human adenovirus serotype 3 (H5/H3). In

282   addition, for transcriptional targeting, the 5' upstream region of the therapeutic gene for

283   roundabout 4 (ROBO4; endothelial specific promoter) was configured within the deleted

284   adenovirus E1A/B site. The integrin targeting peptide RGD4C (CDCRGDCFC) was incorporated

285   into HI loop of Ad fiber knob for transductional targeting.

286   **Figure 2. In *vitro* validation of adenoviral vectors. A,** Assessment of inclusion the HSV*tk*

287   gene into E1 region from purified viral genomes (i Ad5, ii Ad5.CMV.HSVtk and iii triple targeted

288   Ad-HSVtk) by polymerase chain reaction (PCR) using HSVtk specific primers. Viral genomes

289   were shown in black arrow, and amplified HSVtk gene from each of the viral genomes were

290   shown in red arrow. **B,** Validation of HSV*tk* gene delivery and expression *via* Ad vectors in

291   HUVEC cells using western blotting analysis. **C,** Evaluation of cell killing efficiency by

292   HSVtk/GCV treatment on endothelial cells. Each of HUVEC (human) and bEnd-3 (mouse) were

293   infected with each virus encoding either GFP or HSVtk and then treated with Ganciclovir (GCV)

294   prodrug (serial diluted drug concentration shown in x-axis). Results are presented as the relative

295   percentage of cell viability measured by cellular ATP contents. **D,** Assessment of transduction

296   efficacy in *vitro.* Each of NIH/3T3 (mouse embryonic fibroblast) and bEnd-3 (mouse endothelial

297   cell) were infected with triple targeted Ad5-GFP with two different MOI (500 and 1000). Blue:

298   nuclei (stained with DAPI), and green: GFP signal through Ad vectors.

14

299 **Figure 3. Evaluation of vector targeting *via* systemic delivery in murine xenograft models**

300 **(Triple immunodeficient NOD/SCID/IL2Rɣ [NSG] mice). A,** Comparison analysis of targeting

301 capacity with GFP reporter maker by histopathological methods. Experimental procedures for

302 this study was described in material and methods parts in detail. The cryosections of the liver

303 (upper images) and tumor (bottom images) were obtained from each of Ad5 or triple targeted

304 Ad5-GFP injected mice at three days later. All assay were conducted and compared in parallel

305 conditions. Blue: nuclei (stained with Hoechst 33258), Red: mouse CD31/endomucin in the liver,

306 or mcherry signal from the tumor and Green: GFP signal through Ad vectors. **B,** In *vivo*

307 confirmation of triple targeted Ad5-GFP transduction on tumor endothelium. The cryosection of

308 the tumor (Human 786-0 subcutaneous) was obtained from triple targeted Ad5-GFP infected

309 mice (same as Figure 3A), and were subject to immunofluorescence staining analysis with

310 specific antibodies (anti-Cd31/anti-endomucine or anti-PDGFPβ) as an endothelium marker. In

311 the tumor, endothelium and triple targeted Ad5-GFP are co-localized in Yellow. **C,** In *vivo*

312 validation of ectopic gene delivery and transduction with our triple targeted Ad5-GFP. NSG mice

313 were intravenously injected with 1×10^{11} vp of viruses (each of Ad5-GFP or triple targeted Ad5-

314 GFP) and then harvest of all tissues (Liver, Lung, Spleen, Kidney, Heart, Small Bowel,

315 Pancreas, Brain and Muscle) for histopathological assay by immunofluorescence staining. Blue:

316 nuclei (stained with Hoechst 33258), Red: mouse CD31/endomucin. **D,** Evaluation of targeting

317 specificity of our triple targeted Ad5-GFP in the context of SGH SHPC6 subcutaneous tumor

318 (SHPC6: Syrian Hamster Pancreatic Carcinoma). Experimental procedures for this study was

319 accordance as like Figure 3A. Blue: nuclei (stained with Hoechst 33258), Red: mouse

320 CD31/endomucin in the tumor, and Green: GFP signal through triple targeted Ad vectors.

321 Tumor endothelium and triple targeted Ad5-GFP are co-localized in Yellow (arrow).

322 **Figure 4. Assessment of the therapeutic index gains in a metastatic murine models. A,**

323 The immunodeficient NSG mice were intracardiac injected with 5×10^5 786-0 renal carcinoma

15

324   cells (Luciferase/mCherry gene expressed cell line). Three weeks after tumor implantation, NSG

325   mice were intravenously injected with 1×10^{11} vp of viruses [n=8 mice/each of group with

326   Ad5.CMV.GFP, Ad5.CMV.HSVtk and triple targeted Ad-HSVtk], and treated the GCV

327   (50mg/kg/7days by intraperitoneal injection). All mice were monitored the body weight to

328   determine their survival time [>20% loss of initial body weight as a marker for death. The

329   comparative analysis of therapeutic index gains was assessed between the groups by the tumor

330   progression in **B,** and survival time in **C.** The statistical significance of differences between data

331   determined as a *p*-values (**p< 0.05, by Graph Pad Prism v7.0c software). Tumor progression

332   was detected through ROI value (final ROI value divided by initial ROI) by bioluminescence

333   imaging (BLI) analysis, respectively. The final ROI value were only determined with survival

334   mice at the end of study days (at 56 days post-tumor implantation). All mice from

335   Ad5.CMV.HSVtk virus injected group were died at 3 weeks ago due to of hepatotoxicity as

336   shown in **A.**

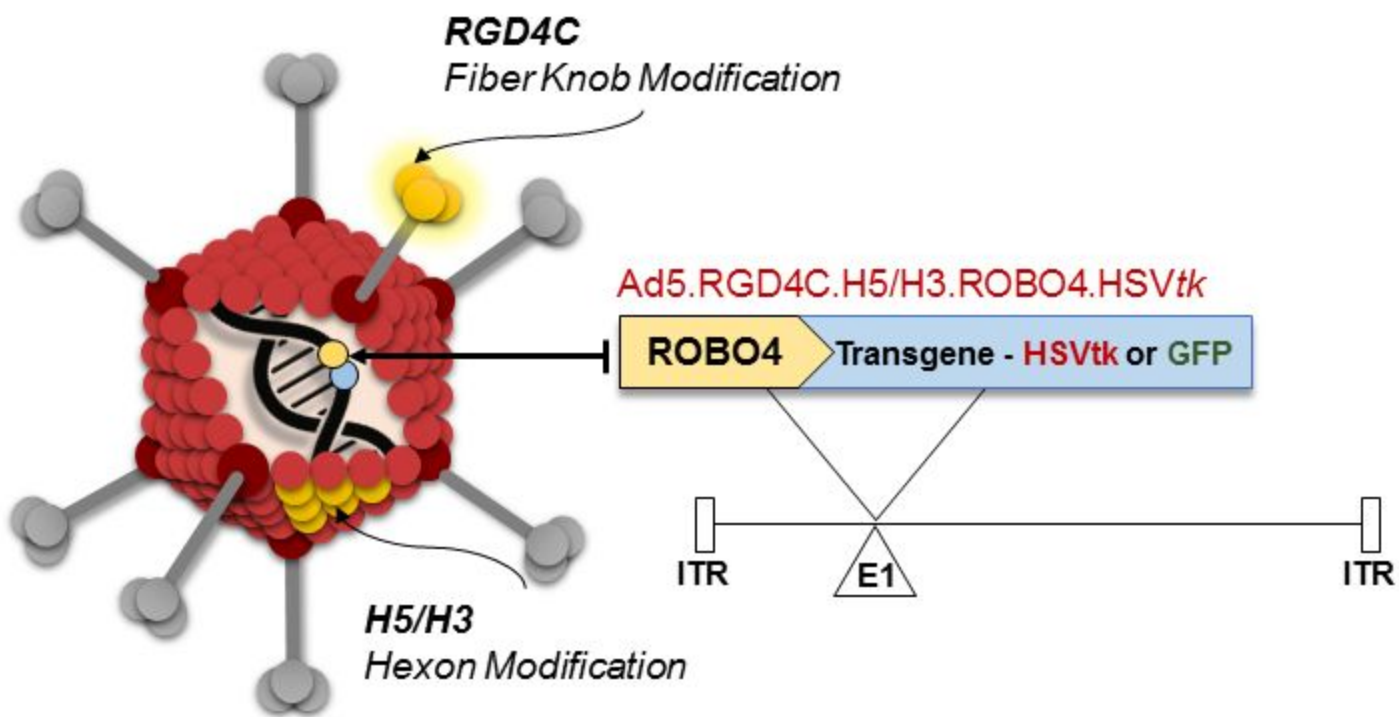16

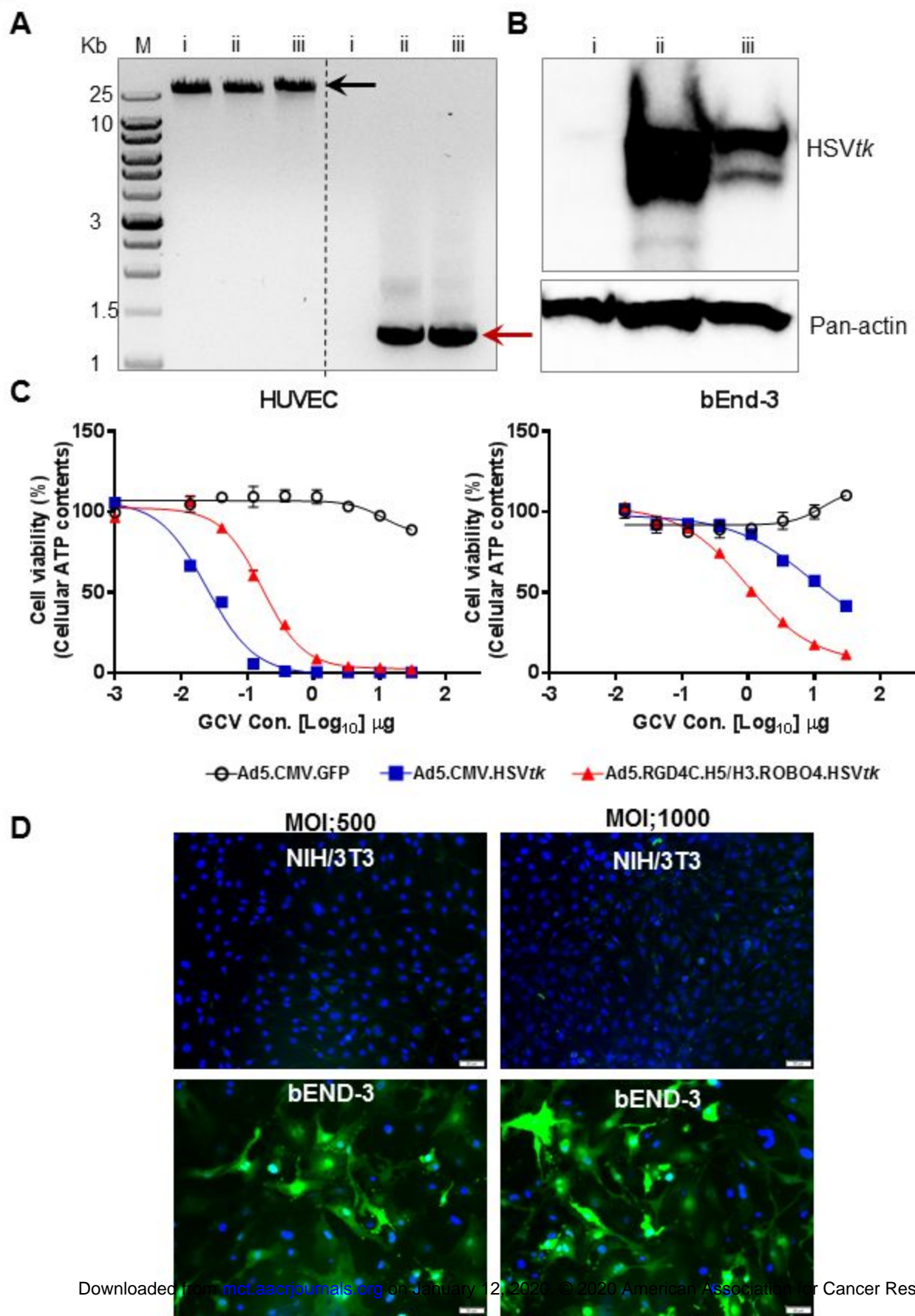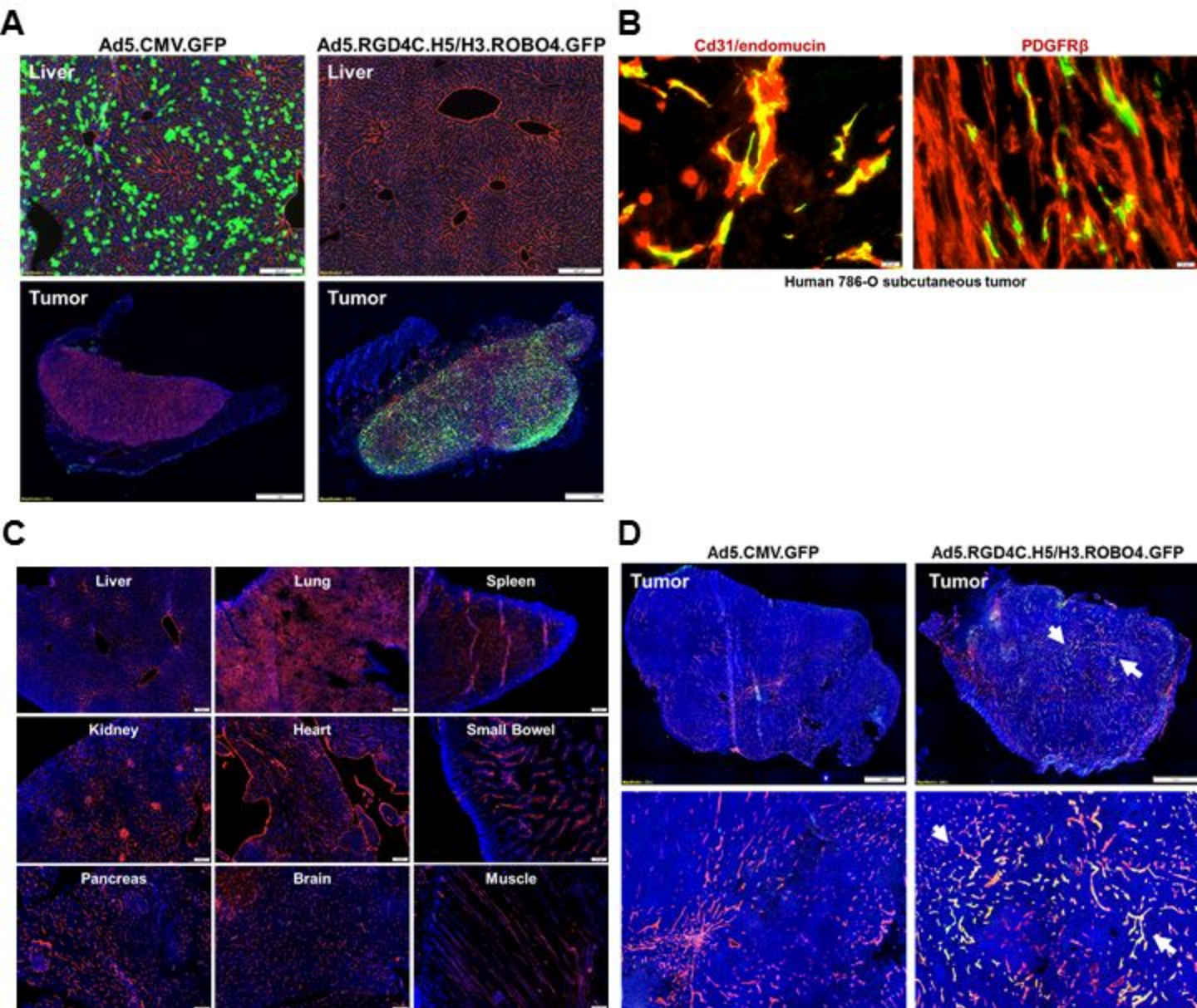# Figure 1

Figure 2

A

HUVEC

B

HSV*tk*

Pan-actin

bEnd-3

C

HUVEC

- Cell viability (%) (Cellular ATP contents)
- GCV Con. [Log$_{10}$] µg

bEnd-3

- Cell viability (%) (Cellular ATP contents)
- GCV Con. [Log$_{10}$] µg

—○— Ad5.CMV.GFP ■ Ad5.CMV.HSV*tk* ▲ Ad5.RGD4C.H5/H3.ROBO4.HSV*tk*

D

MOI;500

NIH/3T3

bEND-3

MOI;1000

NIH/3T3

bEND-3

Figure 3

Figure 4

A

Left panel: Body Weight (% Initial) vs Days — Ad5.CMV.HSVtk + GCV; legend: #6, #11, #12, #13, #15, #24, #29, #31

Right panel: Body Weight (% Initial) vs Days — Ad5.RGD4C.H5/H3.ROBO4.HSVtk + GCV; legend: #4, #8, #9, #14, #18, #20, #21, #28

B Increased tumor (Fold changes) (The final ROI value /initial value); N=8, N=3

C Survival (%) vs Days; ** p<0.005; 3 weeks; Daily GCV treatment (50mg/kg/7times)

-○- Ad5.CMV.GFP   -■- Ad5.CMV.HSVtk   -▲- Ad5.RGD4C.H5/H3.ROBO4.HSVtk
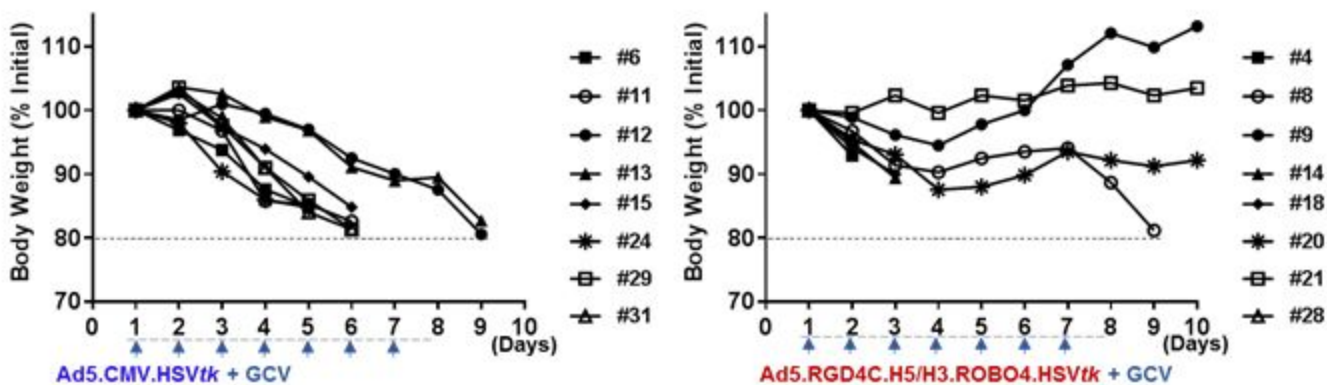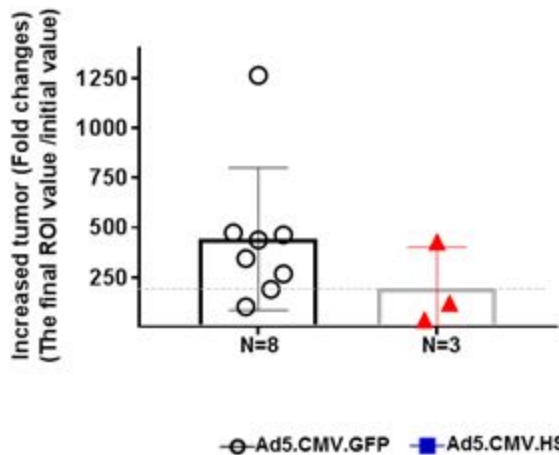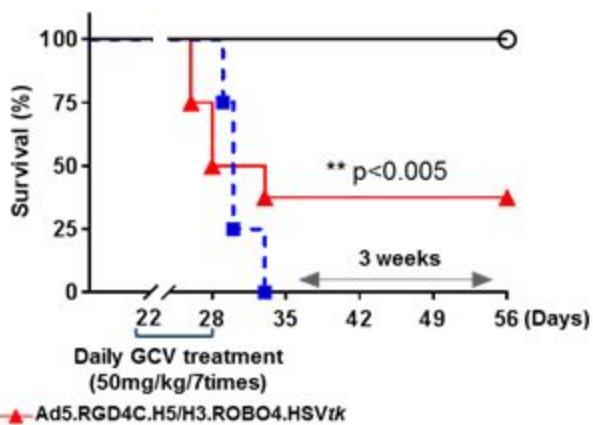
AACR American Association for Cancer Research

Molecular Cancer Therapeutics

Targeting tumor neoangiogenesis via targeted adenoviral vector to achieve effective cancer gene therapy for disseminated neoplastic disease

Myungeun Lee, Zhi Hong Lu, Jie Li, et al.

Updated version	Access the most recent version of this article at: doi:10.1158/1535-7163.MCT-19-0768
Author Manuscript	Author manuscripts have been peer reviewed and accepted for publication but have not yet been edited.

E-mail alerts	Sign up to receive free email-alerts related to this article or journal.
Reprints and Subscriptions	To order reprints of this article or to subscribe to the journal, contact the AACR Publications Department at pubs@aacr.org.
Permissions	To request permission to re-use all or part of this article, use this link http://mct.aacrjournals.org/content/early/2020/01/04/1535-7163.MCT-19-0768. Click on "Request Permissions" which will take you to the Copyright Clearance Center's (CCC) Rightslink site.